

PREPARATION OF TERNARY PANI-MODIFIED TiO₂-HGM NANOCOMPOSITE AND ITS PHOTOCATALYTIC ACTIVITY FOR NITRITE

Y. WU, Y. D. YIN*, X. L. ZHANG, S. C. MA

College of Chemistry and Materials Science, Heilongjiang University, Harbin, China

PANI-modified TiO₂-HGM nanocomposite was successfully prepared through a facile process that combines a sol-gel method and an in situ polymerization method. It exhibited superior photocatalytic activity in nitrite degradation, it can also be easily separated from the reaction system, which solves the problem of difficult recycling. The excellent photocatalytic effect is attributed to the synergistic effect between PANI, HGM and TiO₂. It is higher than that of the commercial P25, and achieving a nitrite degradation rate of 97%.

(Received July 1, 2016; Accepted August 25, 2016)

Keywords: Polymers; Nanocomposites; Nitrite; Photocatalytic activity

1. Introduction

With the growing concern of the energy consumption and environmental pollution, human life and health are facing threaten continuously. Nitrite, one of the common pollutants in drinking water, which could be combined with heme into nitrosamines, is doing harm to our health [1,2]. Titanium dioxide (TiO₂) is considered as the most potentially useful semiconductor photocatalysts because of its high photocatalytic activity, stronger oxidation capacity, relative non-toxicity, high reusable ability, and low cost [3-5]. Due to its bottleneck factors, such as photogenerated hole recombination rate is high, the photocatalytic active reduced as well as the decrease in the number of hydroxyl radicals in the process of photocatalytic [6]; particle size in the nanoscale, which reduces the catalytic activity and difficult to recycle [7], setting an limit to the TiO₂ photocatalyst in the practical process and application fields. Hollow glass microsphere (HGM), due to its buoyancy and good stability, selecting it as the load can not only solve the problem of immobilized nanometer TiO₂ [8], but also realize the photocatalyst regeneration and recycling.

With the deepening of the TiO₂ improvement, good electrical conductivity material gradually entered human sight. Polyaniline (PANI) has been one of the most extensively investigated conducting polymers due to its good stability, nontoxicity, and high instinct redox properties [9]. It has been found that PANI has a forbidden band gap of 2.8 eV, which is suitable to be a sensitizer of TiO₂-based photocatalyst [10]. In addition, PANI accept electronic by photon excitation, inhibition of photogenerated hole to compound, improve the efficiency of photocatalytic quantum [11]. These special characteristics make it a promising material for improving efficiency in the photocatalytic process.

In this study, on the basic of self-made TiO₂ and TiO₂-HGM particles, taken advantage of PANI modified as well as HGM loaded the particles. We choose the nitrite for degradation substrate, and evaluate the photocatalytic activity of PANI-TiO₂-HGM (PTH) from apparent degradation rate and the microstructure characterization.

* Corresponding author: 13613617882@139.com

2. Experimental

2.1 Catalyst Preparation

Nanometer TiO₂ supported on hollow glass microspheres (TiO₂-HGM) were prepared by a sol-gel method. To obtain solution A, 8.5 mL tetrabutyl titanate was dissolved in 19.5 mL ethanol absolute, and the mixture stirred for 30 min, 10 mL acetic acid glacial and 9.7 mL ethanol absolute to obtain homogeneous solution B, then added drop-wise to solution A at room temperature with vigorous stirring for 30 min. HGM was then added to the above solution and mixture was stirred for 30 min. The final solution was further dried until a dry TiO₂-HGM was achieved; this was then placed in a muffle furnace. For comparison, pure TiO₂ was similarly prepared.

In a typical process, 1.25 g ammonium persulfate were dispersed in hydrochloric acid solution under vigorous stirring. After 0.5 h, quantitative of the aniline monomer and TiO₂-HGM were added to the mixture and ultrasonic vibration was continued for another 0.5 h. The reaction continued for 6 h at 0-5 °C under magnetic stirring. The precipitate was centrifuged and washed with deionized water, acetone, and ethanol several times until the washings became colourless. Finally, the product was dried in vacuum at 80 °C for 24 h to obtain the PTH nanocomposites.

2.2 Characterization

The X-ray diffraction (XRD) patterns were collected with a Bruker D8 X-ray Diffractometer using CuK α ($\lambda = 1.5406\text{\AA}$) at step scan of 0.02° from 10° to 80°. The scanning electron microscopy (SEM) images were recorded with a Hitachi S-4800 field emission scanning electron microscope with primary electron energy of (EDX) attached to the SEM was 15 kV. The Energy-dispersive X-ray spectroscopy used to determine the surface elemental composition. The UV-Vis diffuse reflectance spectra were measured using a Scan UV-Vis diffuse reflectance spectrophotometer (TU-1901, China) equipped with an integrating sphere assembly, using BaSO₄ as a reflectance sample.

2.3 Photocatalytic Evaluation

Photocatalytic experiments were conducted in a homemade airtight reactor. A 160 W self-made fluorescent high pressure mercury lamp was used as UV light source. The photocatalyst was suspended in 100 mL of a sodium nitrite solution (0.5 mol/L) under magnetic stirring. The mixture was kept in the dark for 30 min to establish an adsorption-desorption equilibrium before the UV light reaction. At given intervals, 10 mL of suspension was extracted and then centrifuged at 5000 rpm for 5 min to remove the photocatalyst from the supernatant. The absorbance was then measured at 540 nm using a 721 spectrophotometer.

3. Results and discussion

As shown in Fig. 1, the patterns contain nine distinctive TiO₂ peaks at 25.29°, 37.80°, 48.06°, 53.90°, 55°, 62.7°, 68.76°, 70.17° and 75.37°, which are attributed to the crystal planes of (101), (004), (200), (105), (211), (204), (116), (220), and (215), respectively, indicating the formation of the anatase TiO₂ (JCPDS 00-002-0387). Fig. 1 also shows single broad peak of HGM around 22.4° which indicate the presence of amorphous nature. Moreover, PANI-modified TiO₂ particles do not cause any change in peak positions and shapes compared with pure TiO₂. This shows that prepared by 'in situ' polymerization do not change the crystalline structure of TiO₂, which would be very beneficial for photocatalysis of the as-prepared hybrid photocatalyst.

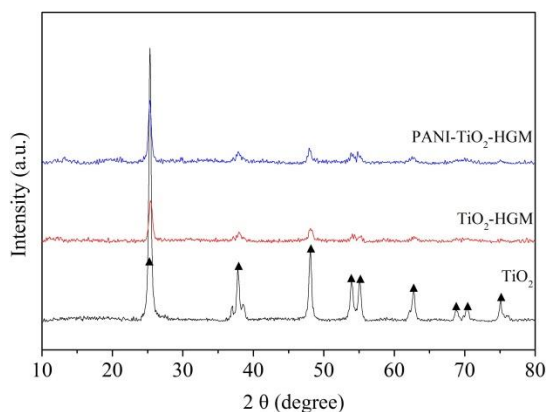


Fig. 1. XRD patterns of different materials

To further verify the composition of ternary PTH by Raman spectra and FT-IR spectra. As shown in Fig. 2A, it was found that the Raman spectrum of pure TiO_2 shows the typical features at 156 cm^{-1} [12]. Further, when PANI was introduced, the Raman spectrum of the resulting PTH displays the typical peaks at 1401 cm^{-1} and 1588 cm^{-1} , which correspond to C–H vibrations in the quinoid/phenyl groups and the semiquinone radical cation structure in molecular PANI respectively. As shown in Fig. 2B, the spectra of PANI mainly included the characteristic absorption bands as following: 1557 cm^{-1} (C=C stretching mode for the quinonoid unit), 1475 cm^{-1} (C=C stretching mode for benzenoid unit). In addition, the bands at about 1294 cm^{-1} is assigned to the C–N stretching mode of the benzenoid ring, while the peak at 1107 cm^{-1} is attributed to the plane bending vibration of C–H, which may be formed by protonation during the polymerization process [13]. The wide peak at $400\text{--}800\text{ cm}^{-1}$ in the spectra of nanocomposite corresponded to the Ti–O bending mode of TiO_2 , which also clearly demonstrate the successful step-wise synthesis of ternary PTH.

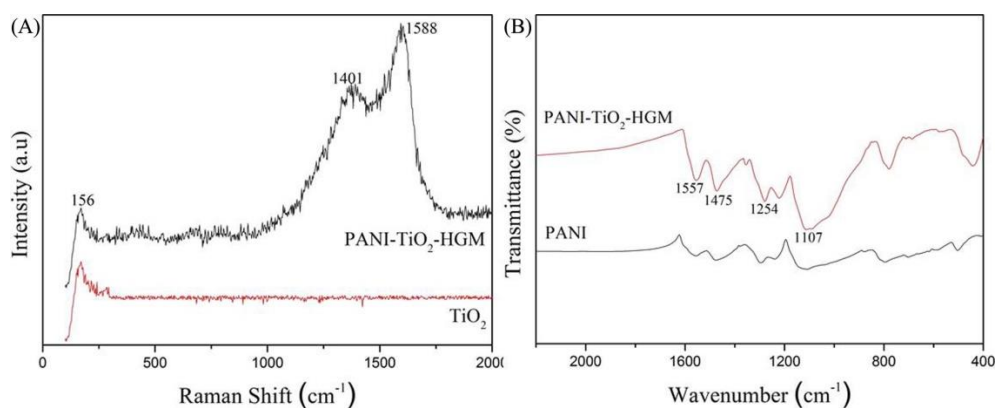


Fig. 2. (A) Raman spectra of TiO_2 and PTH. (B) FT-IR spectra of PANI and PTH

By observing the microscopic characteristics can be seen in Fig. 3, samples are similar to those of TiO_2 on morphology, are all spherical or nearly spherical. But the irregular cracks at the surface of PTH, this is good for pollutants in contact with the catalyst. Take TiO_2 and PTH as examples, both can be seen from the diagram there is no obvious difference on morphology, but

PTH dispersed evenly and TiO_2 agglomerated severely. It is due to TiO_2 nanoparticles size is uniform, high surface energy and surface activity, so the particle is easy to reunite. Instead, because of strong surface effect makes the aniline polymerization on the surface of TiO_2 formed a unique layer upon layer coated ternary bionic structure. This structure has two effects on agglomerate of TiO_2 : PANI polymer chain plays a part in stereo-hindrance effect, blocking the reunion between the particles; on the other hand, doping state of the PANI chain contains a certain amount of positive charge [14], electric double-layer is obviously formed on the particle surface, mutual attraction between the particles offset by the repulsion force between electric double-layer, it is advantageous to the particle dispersion. As shown in Fig. 3c, the presence of Ti can be attributed to TiO_2 ; the presence of Si can be attributed to the HGM; and the presence of oxygen (O) can be attributed to the TiO_2 or HGM. A strong carbon (C) signal can be attributed to PANI in the composite. The EDX pattern suggests a ternary coexistence of PANI, TiO_2 , and HGM in PTH nanocomposite.

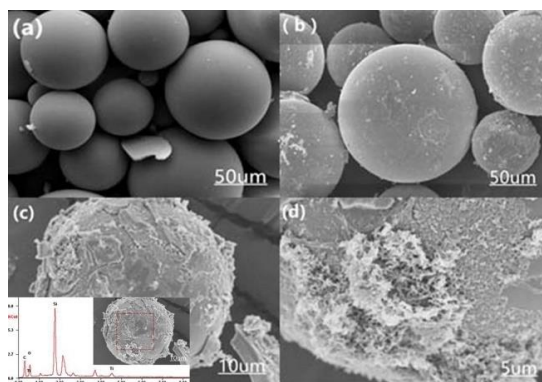


Fig. 3. SEM images of materials: (a) TiO_2 , (b), (c), (d) different size of PTH and EDX spectrum

As seen in Fig. 4, compared with pure TiO_2 , the reflectivity of PTH have significantly lower at 320 nm to 800 nm. The lower reflectivity, the more light energy absorption in the wavelength range, this is helpful to enhance light absorption performance of the photocatalyst. This enhancement not only benefited from the larger specific surface area, but also its irregular surface crack, thus to photons enter into the photocatalyst.

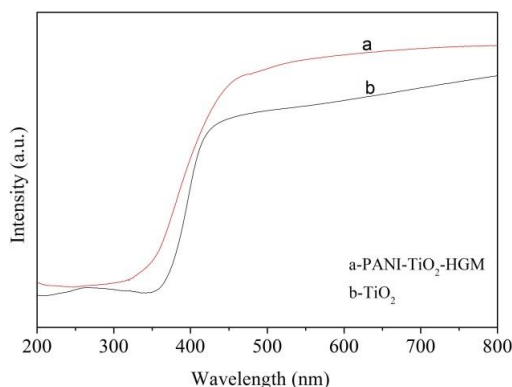


Fig. 4. UV-vis spectra of TiO_2 and PTH.

The photocatalytic performance of ternary PTH photocatalysts is evaluated by degradation of nitrite under UV light irradiation. In Fig. 5A, the degradation efficiency of the different samples was shown to follow the order: $\text{TiO}_2 < \text{TiO}_2\text{-HGM} < \text{P25} < \text{PTH}$. It shows good photocatalytic performance in rate and degree of catalytic degradation. The degradation efficiency of five consecutive cycles is shown in Fig. 5B. As cycling time increasing, the catalytic properties of photocatalyst have not changed significantly. When the first recycling, the degradation rate of nitrite solution slightly dropped from 97% to 95.3%, for the fifth recycling, degradation rate can reach 87.2%. Thus, the PTH has high cycle value.

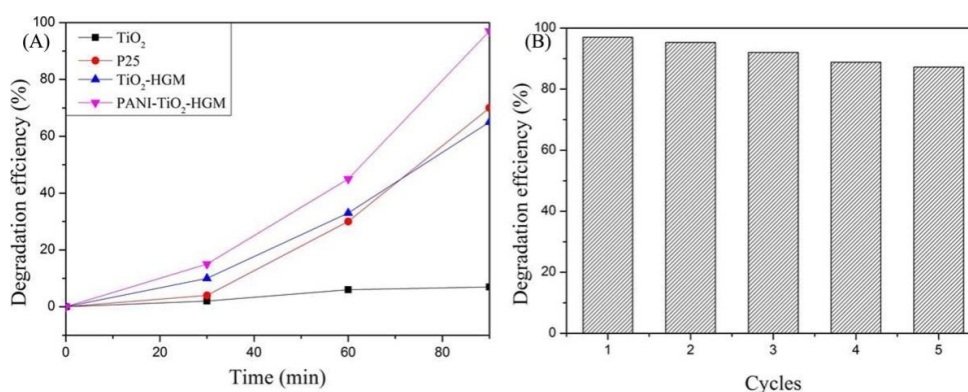


Fig. 5. (A) Effect of different materials on the photocatalytic activity.

(B) Effect of reuse times on the photocatalytic activity

In order to verify the substance is super oxide radicals and/or hydroxyl radicals, which directly involved in the photodegradation process. Put tert butyl alcohol (TBA) and benzoquinone (BQ) in the photodegradation system respectively, which as super oxide radicals scavenger and hydroxyl radicals scavenger [15]. The result is shown in Fig. 6, after joining TBA, the degradation rate of PTH to nitrite only 17.4%. After joining BQ, the degradation rate down to 19.8%. This shows that super oxide radicals and hydroxyl radicals all play an important role in photodegradation process.

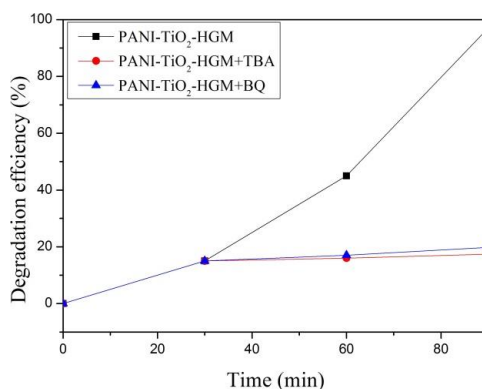


Fig. 6. Photodegradation of nitrite by PTH in the presence of trapping agents

For the PTH photocatalyst, the mechanism could be explained as following: first, the UV light absorptivity was enhanced because of unique layer upon layer coating structure of ternary PTH can facilitate the propagation of light waves and increase the optical path length in photocatalyst by multiple reflections. Second, the high separation efficiency of photogenerated charges could be achieved by the heterojunction built between TiO_2 and PANI. The highest occupied molecular orbital and the lowest unoccupied molecular orbital of PANI were 0.8 V and -1.9 V vs. The valence band and conduction band of TiO_2 was 3.0 V and -0.2 V vs [16]. The energy levels of PANI have been known as well-matched for wide band gap semiconductor TiO_2 . Under UV light irradiation, the heterojunction built between TiO_2 and PANI impelled the excited-state electrons injecting to the conduction band of TiO_2 . Then these excited-state electrons transported to the surface of photocatalyst to react with adsorbed oxygen and water to yield super oxide radicals and hydroxyl radicals, which are responsible for the enhanced photodegradation of nitrite. Last, due to the large specific surface area of HGM, so during the photodegradation of nitrite, it offered more active adsorption sites, which enhanced the interfacial reaction process of photoreaction.

4. Conclusions

In summary, our results succeed for the first time in achieving synchrony of high photocatalytic activity and high recycling rate system. The result shows that modification made by PANI, as well as HGM loaded, can greatly promote the photocatalytic activity of TiO_2 , indicating satisfactory compatibility. It is higher than that of the commercial P25, and achieving a nitrite degradation rate of 97%. Therefore, PTH nanocomposites are promising candidates for the effective photocatalytic treatment of nitrite.

Acknowledgments

The authors are grateful to Science Foundation of Ministry of Education of Heilongjiang Province (12511380).

References

- [1] B.L. Rivas, M.D. Carmen Aguirre, *Reactive and Functional Polymers* **67**, 1471 (2007).
- [2] J.K. Chinthaginjala, L. Lefferts, *Applied Catalysis B: Environmental* **101**, 144 (2010).
- [3] M. Behpour, S.M. Ghoreishi, F.S. Razavi, *Digest Journal of Nanomaterials and Biostructures* **5**, 467 (2010).
- [4] W. Sangchay, K. Ubonchlakat, *Digest Journal of Nanomaterials and Biostructures* **10**, 283 (2015).
- [5] M.G. Brik, Z.M. Antic, K. Vukovic, M.D. Dramicanin, *Mater. Trans* **56**, 1416 (2015).
- [6] Y.X. Li, X.Chen, *Journal of hazardous materials* **227**, 25 (2012).
- [7] V. Loryuenyong, A. Buasri, C. Srilachai, H. Srilachai, *Materials Letters* **87**, 47 (2012).

- [8] K. Ahn, M. Kim, *Journal of Power Sources* **276**, 303 (2015).
- [9] S. Deivanayaki, V.Selvan, *Digest Journal of Nanomaterials and Biostructures* **11**, 115 (2016).
- [10] N.M. Dimitrijevic, S. Tepavcevic, *J. Phys. Chem. C* **117**, 1561 (2013).
- [11] D. Neubert, D. Pliszka, E. Wintermantel, S. Ramakrishna, *Materials Science and Engineering B* **176**, 640 (2011).
- [12] Z.C. Li, L.P. Xing, N. Zhang, Y. Yang, Z.J. Zhang, *Mater. Trans* **52**, 1939 (2011).
- [13] D. Xu, P. Wang, B. Shen, *Digest Journal of Nanomaterials and Biostructures* **11**, 15 (2016).
- [14] X. Pan, C. Qun, Q. Sun, *J. Mater. Chem* **22**, 17485 (2012).
- [15] E.M. Arbeloa, G.V. Procal, S.G. Bertolotti, *Journal of Photochemistry and Photobiology A: Chemistry* **252**, 31 (2013).
- [16] G.K.R. Senadeera, T. Kitamura, Y. Wada, S. Yanagida, *J. Photochem. Photobiol. B* **164**, 61 (2004).